

# One-Pot Synthesis of MoS<sub>2</sub> Flowers Grown On Prussian Blue Cubes For the Sensitive Detection of Catechol In Water Samples

Murugan Keerthi<sup>#</sup>, Vengudusamy Renganathan<sup>#</sup>, Shen-Ming Chen<sup>\*</sup>, Tse-Wei Chen

Department of Chemical Engineering and Biotechnology, National Taipei University of Technology, Taipei, Taiwan 106 (ROC).

\*E-mail: [smchen78@ms15.hinet.net](mailto:smchen78@ms15.hinet.net)

<sup>#</sup>Authors contributed equally.

Received: 30 October 2017 / Accepted: 11 December 2017 / Published: 28 December 2017

---

Herein, we reported a robust electrochemical sensor to detect catechol, developed through the one-pot synthesis of MoS<sub>2</sub> flowers grown on Prussian Blue Cubes. Recently, numerous articles reported about the issue that the water resources were polluted excessively by the chemical and organic toxins. It is a significant concern that the level of toxic compounds exceeds the limits in drinking. Therefore, it is crucial to develop a sensitive, reproducible and long-lasting sensor for the real-time detection of catechol. Thus, we have generated an electrochemical sensor through the economic screen-printed carbon electrode (SPCE) modification method. PB/MoS<sub>2</sub> are economically fabricated on the carbon film of SPCE. As a result, the modified electrode showed exceptional electrocatalytic ability towards catechol, and the redox peak current is associated with the concentrations of catechol. It holds more extensive working range between 25 nM and 1265 μM, and it possesses a very low limit of detection as well as the appreciable sensitivity. This method is successfully applied to the detection of catechol in drinking and river water samples.

---

**Keywords:** Prussian blue cubes; MoS<sub>2</sub> flowers; catechol; water pollutant; organic toxic

## 1. INTRODUCTION

Prussian blue (PB), the octahedral metal hexacyanoferrates with cubic lattice structure[1] gained its extensive consideration in the field of electrochemical sensors owing to its exceptional electron transference[2], excellent electrocatalytic activity[3], high stability, and mainly, due to its distinct conductive[4] and magnetic properties[5]. Prussian blue and its derivatives have been extensively used in the detection of biological molecules[6], hydrogen peroxide[7], nitrite[8], and organic toxins[9]. Also, it has been widely used in supercapacitors[10], batteries[11], energy storage devices[12] and recently in hydrogen storage applications[13]. However, the introduction of

supporting nanomaterials with PB enhances the catalytic functionalization of the material that can be reliably used for sensors. Currently, the transition metal dichalcogenides drew significant consideration due to its unique abilities. Molybdenum disulfide ( $\text{MoS}_2$ ) has exclusive physicochemical properties[14], such as greater surface area, conducting property, and better direct band gaps of 1.2–1.9 eV. These excellent properties tend to be a capable substance for electrochemical sensors[15].

Catechol, an organic compound widely used as a precursor in the manufacture of pesticides, perfumes, and pharmaceuticals. Mainly, Catechol is non-degradable in water. At the same time, massive quantity of wastewater encompassing dyes, and pesticides[16] are released into the freshwater resources[17]. Many articles reported that Catechol is a deadly toxin due to its toxicity and poor degradability[18]. Therefore, we developed  $\text{MoS}_2/\text{PB}$  composite for the electrochemical detection of catechol in water samples. The prepared  $\text{MoS}_2$  flowers grown on PB cubes composites exhibited excellent electrocatalytic ability towards the detection of catechol. The  $\text{MoS}_2/\text{PB}$  film modified screen-printed carbon electrode (SPCE) revealed higher electrochemically active surface area, outstanding electrocatalytic facility[19] and offered extraordinary sensitivity[20] towards catechol.

## 2. EXPERIMENTAL

### 2.1 Materials and Instrumentations

Potassium hexacyanoferrate(II), polyvinylpyrrolidone (PVP, K30), HCl,  $\text{Na}_2\text{MoO}_4 \cdot 2\text{H}_2\text{O}$ , Thiourea were purchased from Sigma-Aldrich and used as received. The SPCEs are purchased from Zensor R&D Co., Ltd., Taipei, Taiwan. The electrochemical measurements were performed using CHI 1205A workstation. The electrochemical studies were carried out in a conventional three-electrode cell using BAS SPCE as a working electrode (area  $0.20 \text{ cm}^2$ ), saturated Ag/AgCl as a reference electrode and Pt wire as a counter electrode. Amperometric measurements were performed with analytical rotator AFMSRX (PINE instruments, USA) with a rotating disc electrode (RDE) having a working area of  $0.24 \text{ cm}^2$ . Scanning electron microscopy studies are performed with (Hitachi S-3000 H). Powder X-ray diffraction studies were performed in an XPERT-PRO diffractometer using Cu K $\alpha$  radiation ( $k=1.54 \text{ \AA}$ ). EIM6ex Zahner is used for electrochemical impedance spectroscopy (EIS) studies.

### 2.2 Synthesis of PB/ $\text{MoS}_2$

Initially, 8.2 g of polyvinylpyrrolidone (PVP, K30) was dissolved in 30 ml of 5mM potassium hexacyanoferrate (II) (pH 1), then 200 ml of HCl was added slowly under magnetic stirring. Then, 160 mg  $\text{Na}_2\text{MoO}_4 \cdot 2\text{H}_2\text{O}$  and 350 mg thiourea was added to the solution and magnetically stirred for 30 min. Then, the solution was taken into a Teflon bomb. Finally, the autoclave was sealed and maintained at  $200^\circ\text{C}$  for 24 h. The gotten precipitate was separated and washed with deionized water and ethanol, then dried under a vacuum drier at ambient room temperature. For comparison,  $\text{MoS}_2$  flowers and PB cubes were synthesized separately.

### 2.3. Fabrication of PB/MoS<sub>2</sub>/SPCE

The active surface area of the screen-printed carbon electrode was pre-cleaned by sweeping in the range between  $-1.0$  V and  $1.2$  V (vs. Ag/AgCl), in pH 5 (0.1 M PB). Next,  $8 \mu\text{l}$  PB/MoS<sub>2</sub> dispersion ( $1 \text{ mg mL}^{-1}$ ) in ethanol was drop cast on SPCE and dried at room temperature.

## 3. RESULTS AND DISCUSSION

### 3.1 Characterizations of PB/MoS<sub>2</sub>

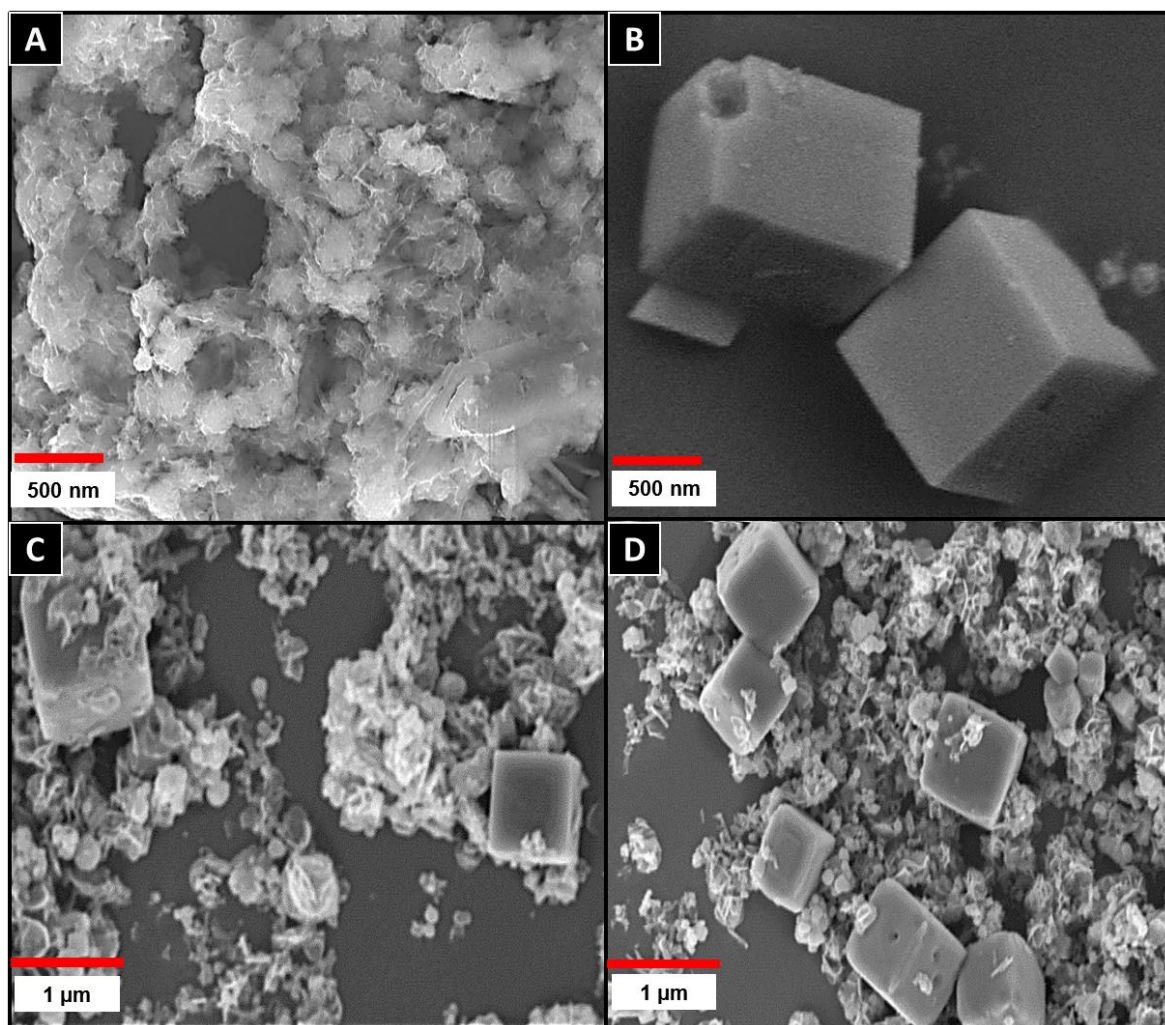


**Figure 1.** SEM images of MoS<sub>2</sub> flowers (A), Prussian blue cubes (B), and PB/MoS<sub>2</sub> composite (C, D)

The synthesized PB/MoS<sub>2</sub> composite was investigated through SEM (Scanning electron microscope), and PXRD (Powder X-ray diffraction).

#### 3.1.1 Morphological characterizations

(Figure 1A) exposes the SEM image of flower-like MoS<sub>2</sub>. (Figure 1B) shows the formation of well-structured PB cubes. (Figure 1C, D) Displays the MoS<sub>2</sub> flowers grown on PB cubes.

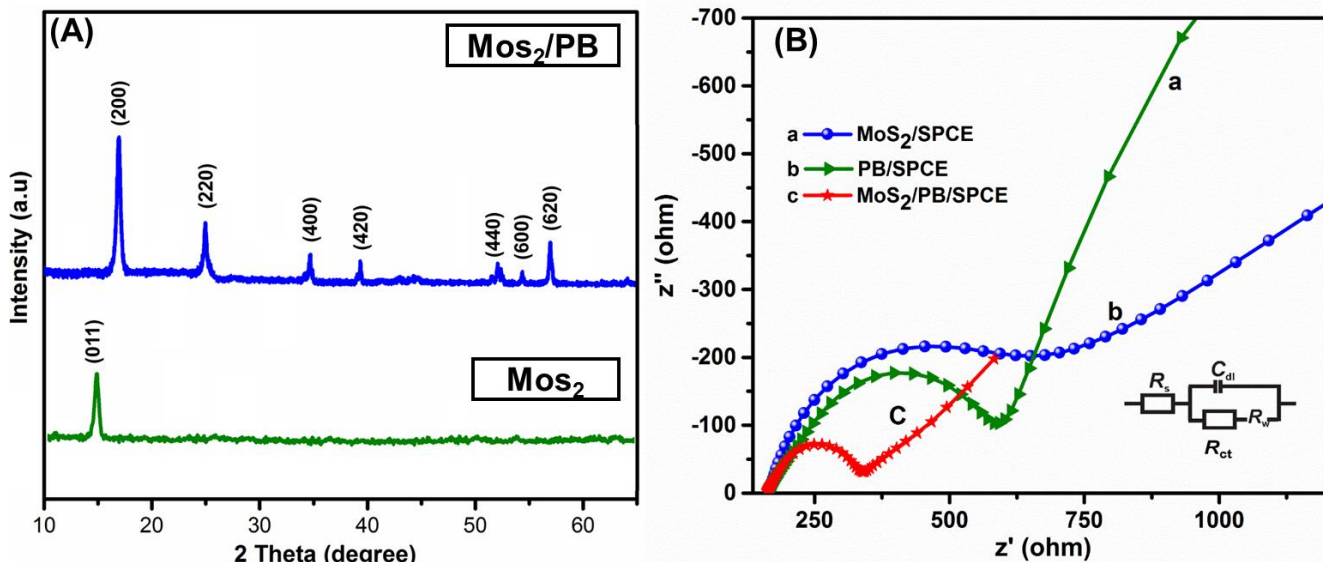


**Figure 2.** (A) PXRD spectra, (B) EIS curves of MoS<sub>2</sub>/SPCE (a), PB/SPCE (b), and PB/MoS<sub>2</sub>/SPCE (c) obtained in 0.1M KCl containing 5 mM Fe(CN)<sub>6</sub><sup>3-/4-</sup>. Inset: Randles equivalent circuit.

3.1.2 PXRD and EIS

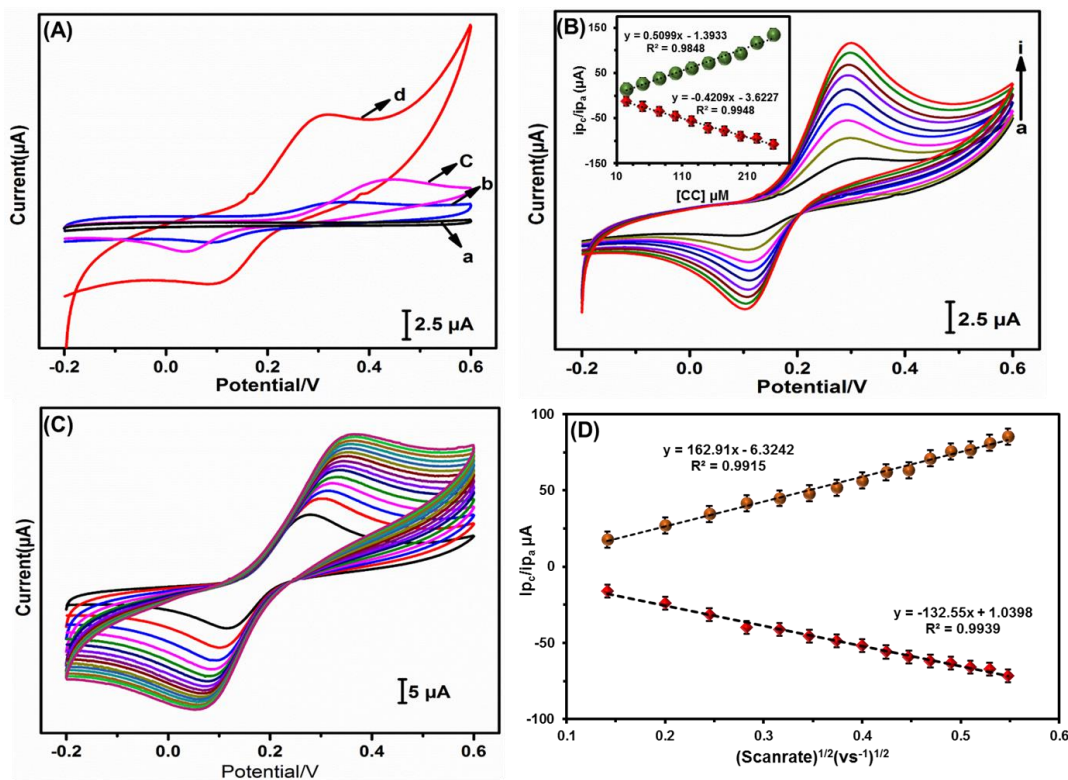


**Figure 3.** (A) CVs obtained for unmodified SPCE (a), MoS<sub>2</sub>/SPCE (b), PB/SPCE (c), PB/MoS<sub>2</sub>/SPCE (d) in 0.1 M Phosphate buffer solution (pH 5) containing 10 μM catechol, scan rate = 50 mV s<sup>-1</sup>. (B) CVs of PB/MoS<sub>2</sub>/SPCE in 0.1 M Phosphate buffer solution (pH 5) containing catechol (a to i; 10 to 90 μM), scan rate = 50 mV s<sup>-1</sup>. [Inset: [CC]/μM vs. current/μA] (C) CVs obtained at PB/MoS<sub>2</sub>/SPCE in 0.1 M Phosphate buffer solution (pH 5) containing 10 μM CC at different scan rates (20 to 250 mV s<sup>-1</sup>). (D) (scan rate)<sup>1/2</sup> (V.s<sup>-1</sup>)<sup>1/2</sup> vs. peak currents (μA).

(Figure 2A) Displays the XRD patterns of MoS<sub>2</sub>, and PB/MoS<sub>2</sub> composite. The PB/MoS<sub>2</sub> exhibited peaks at 16.6° (200), 24.7° (220), 32.8° (222), 37° (400), 38.8° (420), 51.2° (440), 54.7° (600), 57.8° (620). The characteristic peak at 14.8° is assigned to the (011) index of MoS<sub>2</sub>. Gotten PXRD pattern correlates well with that in the literature[21]. Henceforth, the formation of PB/MoS<sub>2</sub> was confirmed. (Figure 2B) displays EIS attained at MoS<sub>2</sub>/SPCE (a), PB/SPCE (b), and PB/MoS<sub>2</sub>/SPCE in 0.1 M KCl comprising 5 mM Fe(CN)<sub>6</sub><sup>3-/4-</sup>. The experimental data acquired by Randles equivalent circuit model[22] (inset to Figure 2B), Where,  $R_{ct}$ ,  $R_s$ ,  $Z_w$ , and  $C_{dl}$  were portraying charge transmission resistance, electrolyte resistance, Warburg impedance[23] and double layer capacitance, respectively. The subsequent order indicates the diameter of semicircles (i.e.,  $R_{ct}$ ); MoS<sub>2</sub>/SPCE (251.3  $\Omega$ ) > PB/SPCE (197.73  $\Omega$ ) > PB/MoS<sub>2</sub>/SPCE (84.48  $\Omega$ ). Provided results shows the lower resistance at PB/MoS<sub>2</sub>/SPCE over other electrodes.

### 3.1.3 Electrocatalyzing ability of PB/MoS<sub>2</sub>/SPCE towards catechol

The CVs obtained at unmodified SPCE (a), MoS<sub>2</sub>/SPCE (b), PB/SPCE (c), and PB/MoS<sub>2</sub>/SPCE (d) in pH 5 (PB) containing 10  $\mu$ M catechol at the scan rate of 50 mV s<sup>-1</sup> between the potential range of -0.2 and 0.6 V was demonstrated in (Figure 3A). The PB/MoS<sub>2</sub>/SPCE displayed greater electrocatalytic capability and reckless electron transmissions as revealed by extremely improved anodic and cathodic peak currents at minimized over-potential. (Figure 3B) displays the CVs obtained at PB/MoS<sub>2</sub>/SPCE in Phosphate buffer (pH 5.0) headed for altered catechol concentrations. The anodic and cathodic peak current increases as the increase in the concentrations of catechol (inset to Figure 3B). The redox peak current improved periodically as the increase in scan rate, which unveiled the signifying electrocatalytic property of the diffusion-controlled electrocatalytic process[24] (Figure 3C). The graphically plotted outcomes between the redox peak current and the square root of scan rate verified the better linearity (Figure 3D).

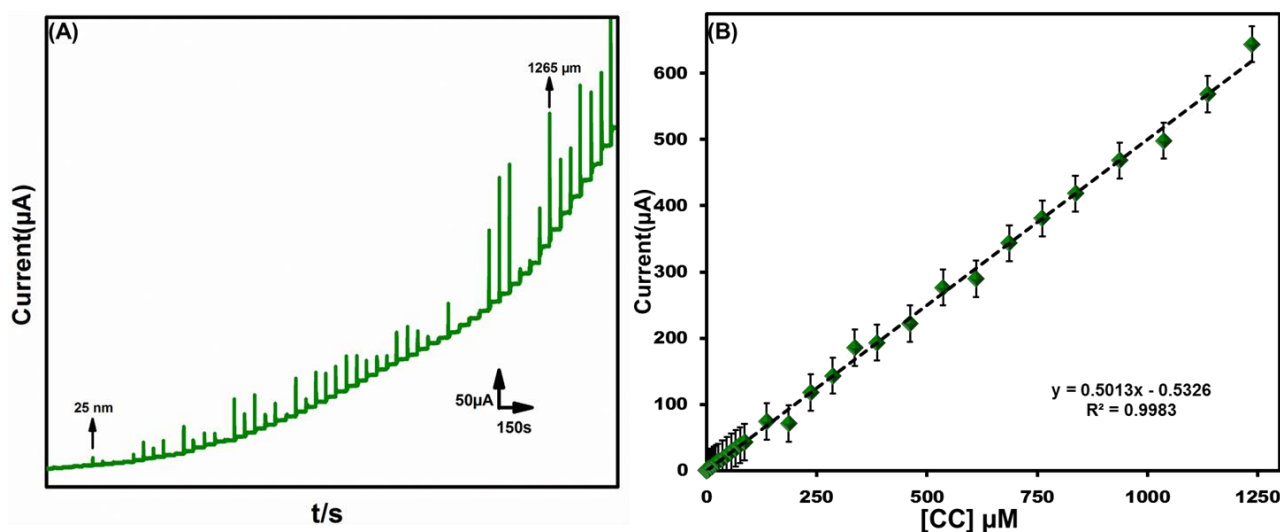


**Figure 4.** (A) Amperometric responses of PB/MoS<sub>2</sub>/RDE for every sequential addition of CC into 0.1 M PB (pH 5). The rotating speed = 1200 RPM. (B) Calibration plot between [CC]/ $\mu$ M and current ( $\mu$ A); working potential ( $E_{app}$ ) = 0.26 V (vs. Ag/AgCl).

**Table 1.** Comparisons of the linear range and limit of detection between the proposed materials for the catechol sensing.

Electrode	LOD/ $\mu\text{M}$	Linear range/ $\mu\text{M}$	Method	Ref.
ZrO <sub>2</sub> /Au	7.68	–	AMP	25
SiO <sub>2</sub> Nanospheres	1.6	12.5 – 450	DPV	26
<sup>a</sup> CD/f/CSA/PEDOT:PSS	0.0275	0.05 – 200	AMP	27
AuNPs/ <sup>b</sup> CS@N, S co-doped MWCNTS	0.2	1–1000	AMP	28
<sup>c</sup> PNR/MCPE	6.4	10 – 100	DPV	29
<sup>d</sup> ERGO/GCE	3.8	6 – 400	DPV	30
<sup>e</sup> aGO <sub>1</sub> /SPCE	0.182	1 – 350	DPV	31
<sup>f</sup> Fc/APTMS/GO	1.1	3 – 112	AMP	32
<sup>g</sup> PM/AuNPs	0.011	0.5 – 175.5	DPV	33
PB/MoS <sub>2</sub> /SPCE	0.06	0.025–1265	AMP	<b>This work</b>

<sup>a</sup>CD/f/CSA/PEDOT:PSS: beta-cyclodextrin with acid-treated poly (3,4 ethylenedioxythiophene) :polystyrene; <sup>b</sup>CS@N,S: Chitosan@Nitrogen, Sulphur; <sup>c</sup>PNR/MCPE: Poly(neutral Red)/Modified carbon paste electrode; <sup>d</sup>ERGO/GCE: Electrochemically reduced graphene oxide/Glassy carbon electrode; <sup>e</sup>aGO<sub>1</sub>/SPCE: activated graphene oxide/screen-printed carbon electrode; <sup>f</sup>Fc/APTMS/GO: Ferrocene/3-Aminopropyl trimethoxysilane/Graphene oxide; <sup>g</sup>PM-AuNPs: Poly(melamine)/Gold nanoparticles.

### 3.1.4 Amperometric determination of catechol

(Figure 4A) Shows the *i-t* curve acquired for PB/MoS<sub>2</sub> composite adapted electrode upon subsequent additions of 0.02  $\mu\text{M}$ , 7  $\mu\text{M}$ , 10  $\mu\text{M}$ , 20  $\mu\text{M}$ , 50  $\mu\text{M}$  and 90  $\mu\text{M}$  of catechol into pH 5 at periodical intermissions of 50 sec ( $E_{\text{app}} = 0.26$  V, vs. Ag/AgCl). Steady and stable results are witnessed on each addition, and the resulting current improved linearly as the catechol concentrations increased

(Figure 4B). Therefore, the linear range is 25 nM to 1265 μM. The limit of detection is 6 nM, and the sensitivity reached 2.3874 μAμM<sup>-1</sup>cm<sup>-2</sup>.

3.1.5 Selectivity towards catechol

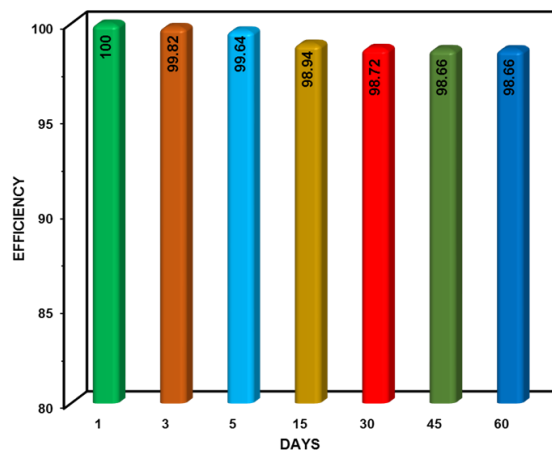


**Figure 5.** Stability of PB/MoS<sub>2</sub>/SPCE as its continuous use for two months. The CV responses of PB/MoS<sub>2</sub>/SPCE towards 10 μM catechol in 0.1 M PB (pH 5), monitored for the given number of days.

The selectivity towards catechol is measured by the amperometric studies with the co-existence of interfering components in water samples. The PB/MoS<sub>2</sub> modified electrode system distributed selective amperometric responses on the addition of 0.005 mM catechol, 50 μM of H<sub>2</sub>O<sub>2</sub>, NO<sub>3</sub><sup>-</sup>, NH<sub>4</sub>OH, and SO<sub>4</sub><sup>2-</sup>. As a final point, the system selectively responded towards catechol in buffer, which is influenced by the mixture of interfering chemicals.

3.1.6 Reproducibility and durability

**Table 1.** Detection of catechol in drinking, and river water samples.

S.NO	REAL SAMPLES	SPIKED (μM)	FOUND (μM)	RECOVERY (%)	RSD (%)
1	Drinking water	3.0	2.92	97.3	2.84
		3.0	5.76	96.0	3.02
2	River water	3.0	2.84	94.6	3.81
		3.0	5.61	93.5	3.37

The prepared electrode’s responses are examined on a daily basis to observe the wearing ability. But, the sensor maintained 98.6% of its first response even after two months although used continuously, authenticated the moral wearing consistency of the proposed electrode. On examining

the reproducibility, CVs are obtained from 5 separate PB/MoS<sub>2</sub>/SPCE in the buffer holding 0.01 mM of catechol; the obtained relative standard deviation is 2.7 %. Stability plot (**Figure 5**) for the electrode is plotted as its sequential usage for two month. The CV responses of PB/MoS<sub>2</sub>/SPCE towards 25 µM catechol in phosphate buffer (pH 5.0) is monitored every day; when it is not in use, it is stored in a refrigerator at 5° C.

### 3.1.7 Real sample analysis

The applied practicality of the system is verified in the samples of drinking water and river water. With the intention of quantifying the catechol in drinking water, identified amount of catechol is spiked into the drinking water under magnetic stirring. Then, the solution is taken as a real sample, and the amperometric method is executed. The electrode distributed fast gestures as laboratory samples. Water corporates want indicative devices to confirm and quantifies the existence of catechol in drinking water. Likewise, this method disclosed virtuous practical applicability in spiked river water samples and the resulting moral parameters were detailed in (Table 1). Satisfying the requirements for the cheap and responsive electrochemical device, here a helpful, as well as an instantaneous analytical tool for the detection of catechol in drinking water and river water samples, is developed.

## 4. CONCLUSIONS

The PB/MoS<sub>2</sub>/SPCE validated an incredibly responsive, reproducible and hard-wearing catechol electrochemical detector. The material was synthesized via simplistic approach, and its practical materialization was publicized by SEM, XRD, EIS and electrochemical methods. The PB/MoS<sub>2</sub>/SPCE exhibited excellent electrocatalytic capability towards catechol detection. The assay procedure was also simple, reckless, and reproducible. This technique tends to be creative in the detection of catechol contained in drinking water and river water samples. In future, it can also be used for the quantification of organic toxins in biological samples.

## ACKNOWLEDGEMENT

The National Science Council and The Ministry of Education, Taiwan supported this work. We would also like to acknowledge The Ministry of Science and Technology, Taiwan (MOST 106-2113-M-027-003) for its financial support.

## References

1. K. Itaya, I. Uchida, V.D. Neff, *Accounts of Chemical Research*, 19(6) (1986) 162-168.
2. Y. Hara, S. Minomura, *The Journal of Chemical Physics*, 61(12) (1974) 5339-5343.
3. A.A. Karyakin, E.E. Karyakina, L. Gorton, *Journal of Electroanalytical Chemistry*, 456(1) (1998) 97-104.
4. S.-i. Ohkoshi, K. Nakagawa, K. Tomono, K. Imoto, Y. Tsunobuchi, H. Tokoro, *Journal of the American Chemical Society*, 132(19) (2010) 6620-6621.
5. S.-i. Ohkoshi, T. Iyoda, A. Fujishima, K. Hashimoto, *Physical Review B*, 56(18) (1997) 11642.
6. J. Li, X. Wei, Y. Yuan, *Sensors and Actuators B: Chemical*, 139(2) (2009) 400-406.
7. A.A. Karyakin, E.A. Puganova, I.A. Budashov, I.N. Kurochkin, E.E. Karyakina, V.A. Levchenko,



- V.N. Matveyenko, S.D. Varfolomeyev, *Analytical Chemistry*, 76(2) (2004) 474-478.
8. L. Wang, S. Tricard, L. Cao, Y. Liang, J. Zhao, J. Fang, W. Shen, *Sensors and Actuators B: Chemical*, 214 (2015) 70-75.
  9. L. Zhang, A. Zhang, D. Du, Y. Lin, *Nanoscale*, 4(15) (2012) 4674-4679.
  10. Y. Zou, Q. Wang, C. Xiang, Z. She, H. Chu, S. Qiu, F. Xu, S. Liu, C. Tang, L. Sun, *Electrochimica Acta*, 188 (2016) 126-134.
  11. V.D. Neff, *J. Electrochem. Soc.* 132 (1985) 1369.
  12. M. Pasta, C.D. Wessells, R.A. Huggins, Y. Cui, *Nature communication*, 3 (2012) 1149.
  13. S.S. Kaye, J.R. Long, *Journal of the American Chemical Society*, 127(18) (2005) 6506-6507.
  14. P. Joensen, R. Frindt, S.R. Morrison, *Materials research bulletin*, 21(4) (1986) 457-461.
  15. S. Kogularasu, M. Akilarasan, T.-W. Chen, S. Selvaraj, *Int. J. Electrochem. Sci.*, 12 (2017) 7435-7445.
  16. V.A. Fitsanakis, V. Amarnath, J.T. Moore, K.S. Montine, J. Zhang, T.J. Montine, *Free Radical Biology and Medicine*, 33(12) (2002) 1714-1723.
  17. P. Fox, M.T. Suidan, J.T. Pfeffer, *Journal (Water Pollution Control Federation)*, 60 (1988) 86-92.
  18. J. Araña, J.D. Rodríguez, O.G. Díaz, J.H. Melián, C.F. Rodríguez, J.P. Peña, *Applied Catalysis A: General*, 299 (2006) 274-284.
  19. S. Kogularasu, M. Govindasamy, S.-M. Chen, M. Akilarasan, V. Mani, *Sensors and Actuators B: Chemical*, 253 (2017) 773-783.
  20. M. Akilarasan, S. Kogularasu, T.-W. Chen, S. Selvaraj, *Int. J. Electrochem. Sci.*, 12 (2017) 7446-7456.
  21. S. Su, X. Han, Z. Lu, W. Liu, D. Zhu, J. Chao, C. Fan, L. Wang, S. Song, L. Weng, *ACS Applied Materials & Interfaces*, 9(14) (2017) 12773-12781.
  22. D.R. Franceschetti, J.R. Macdonald, *Journal of The Electrochemical Society*, 129(8) (1982) 1754-1756.
  23. V. Muralidharan, *Anti-Corrosion Methods and Materials*, 44(1) (1997) 26-29.
  24. F.C. Collins, G.E. Kimball, *Journal of colloid science*, 4(4) (1949) 425-437
  25. P. Bansal, G. Bhanjana, N. Prabhakar, J.S. Dhau, G.R. Chaudhary, *Journal of Molecular Liquids*, 248 (2017) 651-657.
  26. Y. Zheng, D. Wang, Z. Li, X. Sun, T. Gao, G. Zhou, *Colloids and Surfaces A: Physicochemical and Engineering Aspects*, 538 (2018) 202-209.
  27. Y. Qian, C. Ma, S. Zhang, J. Gao, M. Liu, K. Xie, S. Wang, K. Sun, H. Song, *Sensors and Actuators B: Chemical*, 255 (2018) 1655-1662.
  28. H. Rao, Y. Liu, J. Zhong, Z. Zhang, X. Zhao, X. Liu, Y. Jiang, P. Zou, X. Wang, Y. Wang, *ACS Sustainable Chemistry & Engineering*, 5(11) (2017) 10926-10939.
  29. T.S.K. Naik, B.K. Swamy, *Journal of Electroanalytical Chemistry*, 804 (2017) 78-86.
  30. M. Wang, X. Li, J. Liu, W. Xu, Y. Dong, P. Liu, C. Zhang, *Journal of Wuhan University of Technology-Mater. Sci. Ed.*, 32(5) (2017) 1220-1224.
  31. M. Velmurugan, N. Karikalán, S.-M. Chen, Y.-H. Cheng, C. Karuppiyah, *Journal of Colloid and Interface Science*, 500 (2017) 54-62.
  32. M. Elanchezian, D. Manoj, D. Saravanakumar, K. Thenmozhi, S. Senthilkumar *Microchimica Acta*, (2017) 1-8.
  33. S. Palanisamy, S.K. Ramaraj, S.-M. Chen, T.-W. Chiu, V. Velusamy, T.C. Yang, T.-W. Chen, S. Selvam, *Journal of Colloid and Interface Science*, 496 (2017) 364-370.